JNCS Journal of Nepal Chemical Society July 2024, Vol. 44, No. 2, 1-12
ISSN: 2091-0304 (print)
DOI: https://doi.org/10.3126/jncs.v44i2.68263
RESEARCH ARTICLE

# Study of the Molecular Structure, Spectroscopic Analysis, Electronic Structures and Thermodynamic Properties of Niacin Molecule Using First-principles

**Chandra Budha[1], Krishna Bahadur Rai[1*]**

[1]*Department of Physics, Patan Multiple Campus, Lalitpur, Tribhuvan University, Nepal*

[*]*Corresponding E-mail: krishnarai135@gmail.com*

*(Received: April 9, 2024; revised: June 24, 2024; accepted: June 25, 2024)*

## Abstract

This work describes the different properties of Niacin's molecule using the density functional theory (DFT) B3LYP/6-311++G (d, p) basis set. The optimized energy for the Niacin molecule is -436.987 Hartree. The peak values from FT-IR spectra show the C=C, C-C vibrations, C-H stretching vibrations, C-H in-plane bending vibration, C-H out-of-plane bending vibration, C-O stretching vibration, C-N vibration and O-H vibration. The MEP and ESP analyses indicate that the oxygen and nitrogen atoms exhibit nucleophilic regions, while the hydrogen atoms exhibit electrophilic regions. The energy gap of the Niacin molecule is found to be 5.398 eV through HOMO-LUMO analysis. The electronegativity value of 4.847 eV signifies the molecules ability to attract electron and the calculated value of chemical hardness is 2.7 eV which reflects the molecular stability. The softness value of 0.370 $eV^{-1}$ denotes the molecule polarizability. Also the chemical potential value is -4.847 eV which represent the ability to donate or accept electron. Similarly, electrophilic index with value 4.351 eV shows the electrophilic behavior that signifies its capacity to accept electron. Because of the larger energy gap, the molecule becomes hard and hardness is greater than softness. In this molecule, the C2 atoms have the highest positive charge along with C3 and all the hydrogen atoms, while C1 has the highest negative charge together with some negative charge on C4, C5, N6, C11, O12 and O13 atoms. When the temperature rises, the thermodynamic parameters such as heat capacity at constant volume and pressure, internal energy, enthalpy, and entropy increase, but Gibbs free energy decreases.

**Keywords:** Niacin; Density Functional Theory; Vibrational analysis; Electronic structure; Thermodynamic parameter

## Introduction

Niacin has the carboxylic acid group (-COOH), which determines its chemical properties and its important role is in both synthetic organic chemistries and biochemical functions. So, it is a functional group that lies in coenzymes nicotinamide adenine dinucleotide (NAD) and nicotinamide adenine dinucleotide phosphate (NADP). There are 14 atoms and 64 electrons in Niacin molecule. **Fig. 1** shows the chemical structure of Niacin molecule. It has multiple roles in oxidative processes by helping energy metabolism and deoxyribonucleic acid (DNA) repair, which is commonly known as nicotinic acid or vitamin $B_3$ and the International Union of Pure and Applied Chemistry (IUPAC) name is pyridine-3-carboxylic acid. In 1937 it was first discovered as the medicine to prevent black tongue disease in dogs and treatment for pellagra disease [1]. Water soluble vitamin $B_3$



©Nepal Chemical Society

called Niacin is also an essential human nutrient and has an important role other than vitamin in cholesterol and lipoprotein metabolism [2]. It is a white, odorless, crystalline solid and also soluble in alcohol and it is stable in the presence of the usual oxidizing agent [3]. Vitamin $B_3$ can be obtained from both endogenous (i.e. found in foods like milk, yogurt, red meat, fish, poultry, etc.) and exogenous (i.e. found in foods like vegetables and animals) sources [4]. It has several effects, including raising high-density lipoprotein (HDL) cholesterol, increasing vascular remodeling, reducing inflammation, and also used as therapy for neurological injury and diseases [5]. The properties of Niacin have been investigated in a number of recent works employing the Gaussian 09W density functional theory (DFT) technique with B3LYP/6-311++G (d, p) basis set [6]. Niacin's behavior in oil and water environments was studied by using DFT and they found that configurations with both up and down orientations that provide the maximum stability in water, whereas configurations in oil and gas phases show somewhat lower stability [7]. DFT was used to examine crystal formation, including crystals and single-crystal X-ray diffraction, and to clarify geometric structure optimization [8]. Bardak used molecular docking, Fukui analysis, and DFT calculations to investigate the impact of active atoms specifically, the carboxyl group and nucleophilic atoms on the bioactivity of Niacin derivatives [9]. The study involved examining the inelastic neutron scattering spectra of nicotinic acid, applying DFT to understand its vibrational modes and intermolecular interactions, and verifying the stability of nicotinic acid at low temperatures using both experimental and theoretical data [10]. Monte Carlo strategies for the First-Principles calculations are widely employed for investigating electronic structure and ascertaining diverse properties [11].

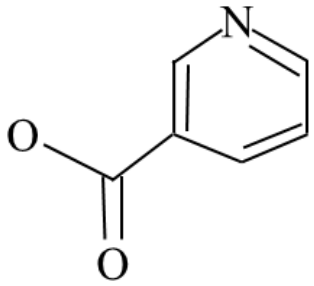


***Figure 1****: Chemical structure of Niacin molecule*

This research investigates better understanding of the Niacin molecule's functional group and their role in biological process such as cellular metabolism, lipid metabolism, DNA maintenance and neurological function. For Niacin, understanding the electron density distribution around the pyridine ring and carboxyl group explain how it interacts with enzymes and other biomolecules. HOMO-LUMO gap suggest its potential to participate in redox reactions. Frontier molecular orbitals indicate the sites of chemical activity on the Niacin molecule and this is crucial for understanding how Niacin acts as a precursor to coenzymes involved in redox reactions. In this study, we are going to find out the optimized structure, molecular vibrational, electronic structures like molecular electrostatic potential (MEP), electron density (ED), electrostatic potential (ESP), highest occupied molecular orbital-lowest unoccupied molecular orbital (HOMO-LUMO) energy gap, density of states (DOS), global reactivity and Mulliken atomic charges using DFT at B3LYP/6-311++G (d, p) basis set. In addition to these, we are also investigating the thermodynamic properties. So, by analyzing electronic properties, orbital gap energies, and other global chemical descriptors, a deeper understanding about the Niacin biological functions

is gained. These insights can lead to a more detailed explanation of its roles in metabolic processes, enzyme interactions, and overall bioactivity, providing a more comprehensive picture of its biological significance.

## Computational Methodology

The molecular geometry of the Niacin molecule was performed in DFT (Gaussian09W program) at the Becke's three parameter (local, non-local, Hartree Fock) hybrid exchange function with Lee- Yang Pair (B3LYP)/6-311++G (d, p) basis set for all the quantum chemical calculations. In this basis set, the molecule's optimized structure, optimization steps number, vibrational spectroscopic (i.e. FT-IR spectrum), MEP, ED, ESP, HOMO-LUMO energy gap, global reactivity and Mulliken charges were determined. GaussView 6.0 is a graphical user interface used in conjunction with Gaussian software for computational chemistry. GaussView simplifies the process of creating input files for Gaussian, visualizing the results of Gaussian calculations, and analyzing molecular structures and properties. GaussSum3.0 software was used to visualize and calculate the DOS. Thermodynamic properties were obtained from the output .log file after inserting on the Moltran software. Also OriginPro 9.0 software was applied to plot the graph from the data obtained of the $C_6H_5NO_2$ molecule.To calculate the global reactivity parameters like ionization potential ($I = -E_{HOMO}$), electron affinity ($A = -E_{LUMO}$) values, hardness (η), softness (S), chemical potential (μ), electronegativity (χ), global electrophilicity or electrophilicity index or electrophilic index (ω), we use Koopman's theorem [12, 13], in which

$$\text{Chemical hardness } (\eta) = \frac{1}{2}(I-A) \quad (1)$$

$$\text{Softness } (S) = \frac{1}{\eta} \quad (2)$$

$$\text{Chemical potential } (\mu) = -\frac{1}{2}(I+A) \quad (3)$$

$$\text{Electronegativity } (\chi) = \frac{1}{2}(I+A) \quad (4)$$

$$\text{Electrophilic index } (\omega) = \frac{\mu^2}{2\eta} \quad (5)$$

## Results and Discussion

### Optimized Molecular Geometry

The optimized stabilized energy is the minimum energy required for the molecule to be in stable. Therefore, the molecule is stable and has the lowest ground state energy while it is in the optimized state. **Fig. 2(a)** shows the minimum energy configuration or the ground state optimized geometry of the Niacin molecule along with symbol and numbering of atoms. The initial input structure of Niacin was created using GaussView6.0. **Fig. 2(b)** represents the total energy optimization process of the Niacin molecule and it attains its optimized energy at -436.987 Hartree (-11891.028 eV).

### Vibrational analysis of Niacin molecule in FT-IR spectrum

**Fig. 3** shows the FT-IR-spectra of Niacin molecule. There are 14 atoms in the $C_6H_5NO_2$ molecule having 36 modes of vibration (3N-6 modes of vibration) in which it contains 25 in-plane vibrations, (A′ = 2N-3) and 11 out-of-plane vibrations, (A″ = N-3) [14, 15]. The C=C mode of vibration occurs in the range of 1400-1650 $cm^{-1}$ and C-C vibration is found to be in the range of 1350-1420 $cm^{-1}$ [16]. In our $C_6H_5NO_2$ molecule, **Fig. 3** displays the C=C vibration peaks at 1448 and 1632 $cm^{-1}$ and C-C vibrations is at 1358 $cm^{-1}$ in the FT-IR spectrum. For hetero aromatic structures, the C-H stretching mode of vibration is generally weak and in the range of 3000-3300 $cm^{-1}$ [17]. In our title molecule, the observed C-H stretching vibrations are 3152, 3184 and 3202 $cm^{-1}$ in the FT-IR spectrum peak. C-H in-plane bending vibration ranges from 1000-1300 $cm^{-1}$ and C-H out-of-plane bending vibration ranges from 675-1000 $cm^{-1}$ [16, 17]. The observed values of

C-H in-plane bending vibrations are occurred at 1040, 1112 and 1208 $cm^{-1}$, and C-H out-of-plane bending vibrations exist at 712, 760, 792 and 884 $cm^{-1}$ in FT-IR spectrum. The C=O stretching vibration bands are in the range of 1680-1715 $cm^{-1}$ [17].

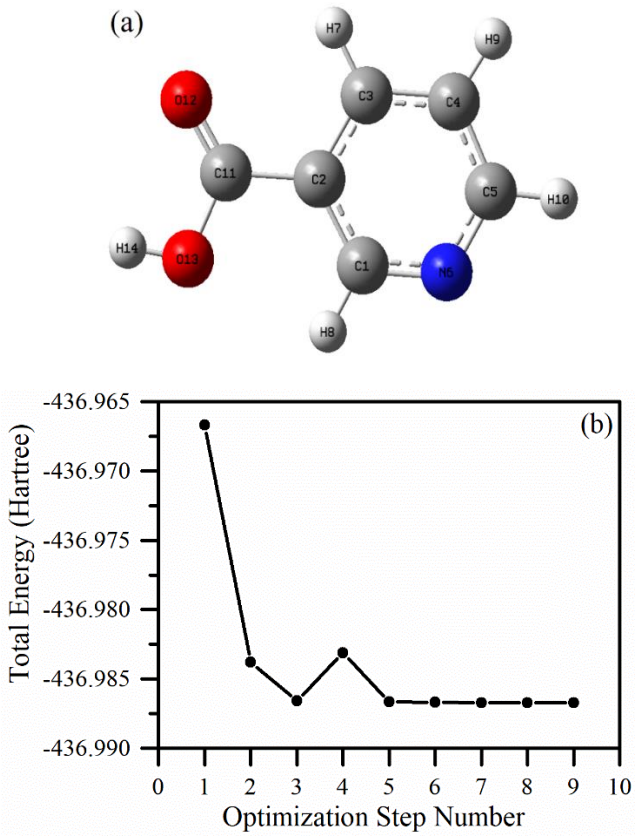


***Figure 2:*** *(a) Optimized structure of Niacin molecule with symbol and numbering of atoms, (b) plot for optimization step number vs total energy*

In our molecule, the observed peak vibration of the FT-IR spectrum is at 1792 $cm^{-1}$. By the missing of many bands, it is difficult to introduce the CN vibration, the CN (C=N and C-N) mode of vibration is in the range of 1234-1564 $cm^{-1}$ [18]. In this study, the observed vibrations are 1292 and 1449 $cm^{-1}$ as shown in Figure 3 of the FT-IR spectrum. The O-H mode of vibration is generally weak due to the presence of intermolecular hydrogen bonding in the range of 3580-3670 $cm^{-1}$ in the unassociated hydroxyl group [19]. In the $C_6H_5NO_2$ molecule, we observe O-H vibration peak at 3768 $cm^{-1}$ in FT-IR spectrum. The vibrations frequencies obtained from this research are in good agreement with the values from the article [20]. DFT-predicted vibrational bands corresponds to the functional groups in Niacin (e.g., carboxyl group, pyridine ring). To understand the proper uses of the spectral interpretations in biological roles of functional groups, it requires vibrational frequencies together with the understanding of interactions and specific structural and then functional roles of Niacin's functional groups in a biological environment. DFT can predict the equilibrium structure of Niacin in its ground state, providing insight into bond lengths, angles, and electronic distribution [21].

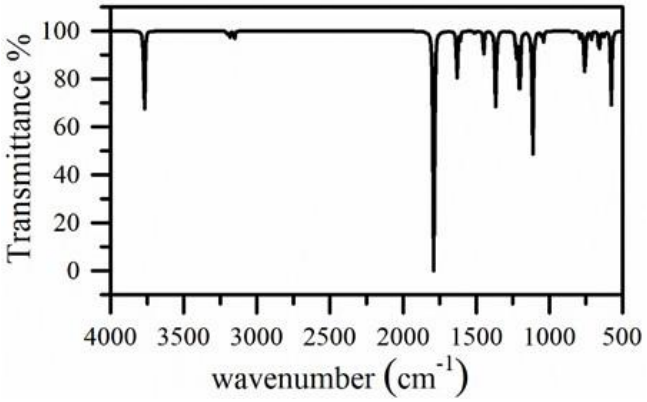


***Figure 3****: FT-IR-spectra of Niacin molecule*

**Molecular Electrostatic Potential (MEP) and Electron Density (ED) analysis**

MEP is the property of the molecule that creates an electrical potential at each point in the surrounding space. **Fig. 4(a)** represents the MEP map with potential value ranges from red < orange < yellow < green < blue color lying in between -6.143e-2 a.u. to 6.143e-2 a.u. scale. Electrophilic reactivity occurs at the negative region of electrostatic potential and nucleophilic reactivity occurs at the positive region of electrostatic potential [22]. Also, the MEP surface displays the molecule's size, shape and

electrostatic potential values [23]. Red color represents the negative region which is for the electrophilic attraction and blue color represents the positive region and is preferred site for nucleophilic attraction [24]. In this molecule, we found that oxygen and nitrogen atoms show the nucleophilic region (yellow color) and the hydrogen atom shows the electrophilic region (blue color). The numeral value of Mulliken charges are matched with electrophilic and nucleophilic region. **Fig. 4(b)** shows the electron density (ED) map and it presents the formation of electron bond distribution and also describes the bonding interaction.

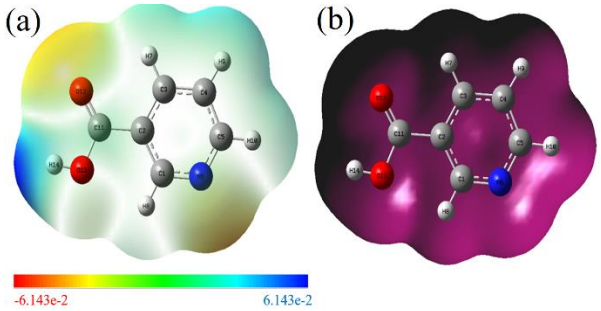


***Figure 4:*** *(a) Molecular electrostatic potential, (b) Electron density of Niacin molecule*

**Electrostatic Potential (ESP) analysis**

**Fig. 5(a)** represents the solid figure and **Fig. 5(b)** represents the transparent figure of electrostatic potential of Niacin molecule with the observed potential ranges from -1.119e-2 to 1.119e-2 a.u. denoted by different color ranges i.e. red < orange < yellow < green < blue. The information on electronegativity and partial charge of the molecule can be seen in the ESP map. The reactivity and their chemically active sites of atoms are represented visually by ESP [25]. It is used to analyze the distribution of potential in connection with different colors of the bonded atom in the molecule [26]. Red color represents the negative region (i.e. electrophilic attract) and blue color represents the positive region (i.e. nucleophilic attract) [27]. In our molecule, oxygen and nitrogen atoms are in negative region which is electrophilic attract site and all the hydrogen atoms are in positive region which represent the nucleophilic attract site. In biochemical reactions, the oxygen atom in the carboxyl group (-COOH) of Niacin acts as a nucleophilic site. This is evident in esterification reactions where the carboxyl oxygen attacks an electrophilic carbon center [28, 29]. The nitrogen atom in the pyridine ring of Niacin also acts as a nucleophilic site in various biochemical pathways, such as NAD+ formation [28, 30]. In hydrogen bonding interactions, hydrogen atoms bonded to electronegative atoms like oxygen and nitrogen in Niacin participate as electrophilic sites. These hydrogen atoms are attractive to nucleophiles, as seen in hydrogen bonding with water molecules or other biological molecules [28, 31].

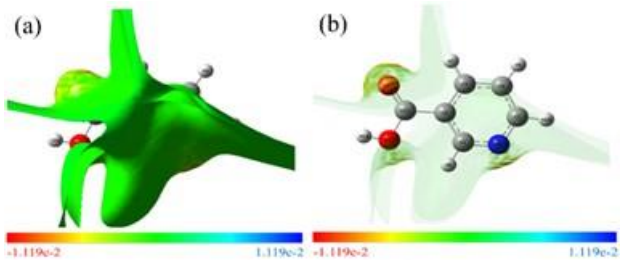


***Figure 5****: Electrostatic potential of Niacin molecule (a) solid, (b) transparent view*

**HOMO and LUMO Analysis**

The highest energy (outermost) orbital carrying an electron to donate is called the highest occupied molecular orbital (HOMO) and the lowest energy (innermost) orbital to accept an electron (i.e. electron acceptor) is called lowest unoccupied molecular orbital (LUMO) so that ionization potential and electron affinity are directly associated with the energy of HOMO and LUMO [32]. The energy difference between HOMO and LUMO is known as the energy gap [33]. The molecule reactivity increases while decreasing the energy gap ($\Delta E = E_{LUMO} - E_{HOMO}$)

which leads to an increase in the occupancy ability of the molecule [34]. If the value of the energy gap is higher, then the electronic transition is lower and vice versa [16, 17]. If the energy gap is a positive value, then the molecule is stable and if the energy gap is a negative value, it becomes unstable. **Fig. 6** shows the HOMO and LUMO with their respective energy values for the $C_6H_5NO_2$ molecule. In this work, the energy of HOMO and LUMO are found to be -7.546 eV and -2.148 eV respectively. Thus it is observed that the energy gap of the $C_6H_5NO_2$ molecule is 5.398 eV from the energy of HOMO-LUMO. The MEP, ESP and HOMO-LUMO analysis match the value obtained from the article [35].

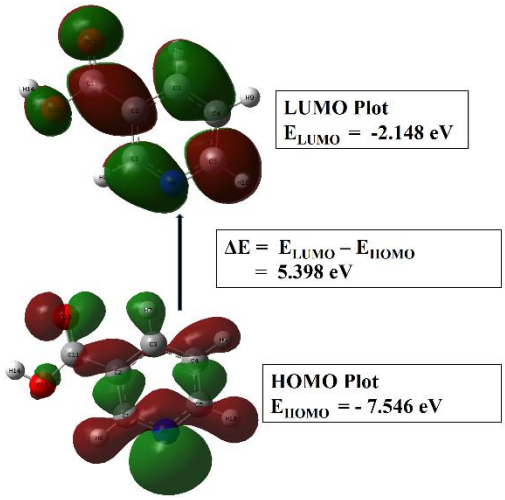


***Figure 6**: HOMO – LUMO energy difference of Niacin molecule*

**Global Reactivity**

Utilizing ionization potential ($I = -E_{HOMO}$) and electron affinity ($A = -E_{LUMO}$) values enable the derivation of various global parameters including hardness (η), softness (S), chemical potential (μ), electronegativity (χ), global electrophilicity or electrophilicity index or electrophilic index (ω). Hardness represents a chemical system's resistance to electron cloud deformation caused by external perturbations during a reaction, closely tied to its stability and reactivity. Softness, conversely, stands as the inverse of hardness, provides additional insight into this resistance. The chemical potential (μ) of a molecule signifies its aptitude for engaging in chemical reactions or undergoing chemical changes. Electronegativity (χ) aids in determining the potential energy released or absorbed during a reaction. Electrophilicity index (ω) indicates a molecule's ability to accept electrons, aiding in predicting its reactivity toward nucleophiles in chemical processes [12]. To calculate the global reactivity parameters of the molecule, we use ionization potential i.e. $I = -E_{HOMO}$ = 7.546 eV and electron affinity i.e. $A = -E_{LUMO}$ = 2.148 eV. Using equation (1) to (5), we get the Chemical hardness (η) = 2.7 eV, Softness (S) = 0.370 $eV^{-1}$, Chemical potential (μ) = - 4.847 eV, Electronegativity (χ) = 4.847 eV, and Electrophilic index (ω) = 4.351 eV. It is clear that the molecule is very hard because it has a large HOMO-LUMO gap (5.398 eV), also the value of hardness (2.7 eV) is greater than the value of softness (0.370 $eV^{-1}$). The electronegativity with the value 4.847 eV indicates the tendency of an atom within a molecule to attract the shared pair of electrons towards itself and the chemical potential (-4.847 eV) represents the ability to donate or accept electrons. Electrophilic index having 4.351 eV shows its capacity to accept electron in chemical reaction. All the global reactivity values are in well agreement with values obtained from the article [35].

**Density of States (DOS) Analysis**

By employing DOS, electrons are replicated from the valance band to the conduction band [36]. There are several steps possible for occupation at high-intensity DOS and anti-bonding interaction occurs at the negative intensity DOS, while there is no states in zero-intensity DOS [17, 37]. From **Fig. 7**, the observed energy gap of HOMO–LUMO in the density of state is 5.429 eV. From DOS spectrum and HOMO-

LUMO energy, we have observed the energy gaps are 5.429 eV and 5.398 eV respectively and these energy gaps obtained from DOS spectrum and HOMO-LUMO energy are approximately equal

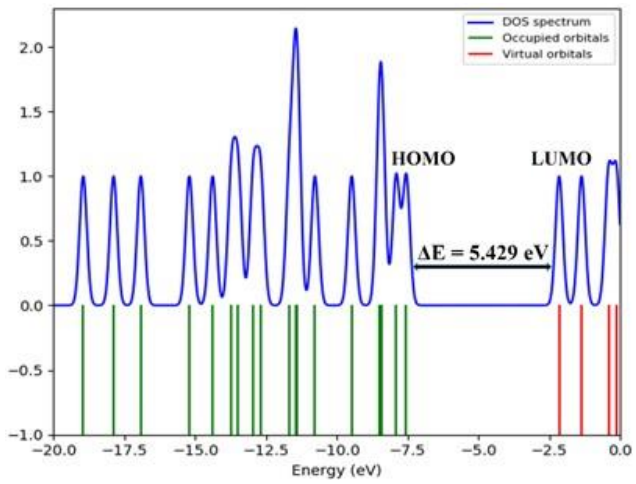


***Figure 7**: Density of states of Niacin molecule*

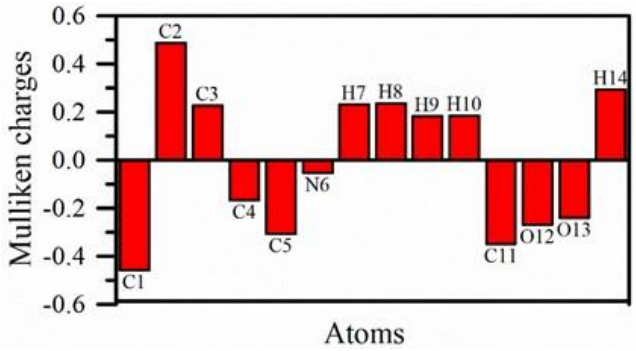


***Figure 8**: Histogram of Mulliken charges distribution of each atom in Niacin molecule*

**Mulliken Atomic Charge Distribution**

Mulliken atomic charges play an important role in determining the electronegativity of s-, p-, and d- states by quantum chemical calculation [38, 39]. Also with the help of Mulliken's charge, the net atomic population of the compound can be determined. When two atoms are bound together, the total overlap population is positive and when they are anti-bonded, it is negative [40]. **Fig. 8** shows the calculated Mulliken charges distribution value of Niacin molecule. It can be observed that C2, C3, H7, H8, H9, H10 and H14 atoms of Niacin molecule show positive charge indicating electrophilicity behavior and C1, C4, C5, N6, C11, O12 and O13 show negative charge indicating nucleophilicity behavior. Among them, C2 atom has the highest positive charge and C1 atom has the highest negative charge. Mulliken method is still widely used due to its simplicity even though it doesn't consider polarization effect in molecule which yields incorrect result.

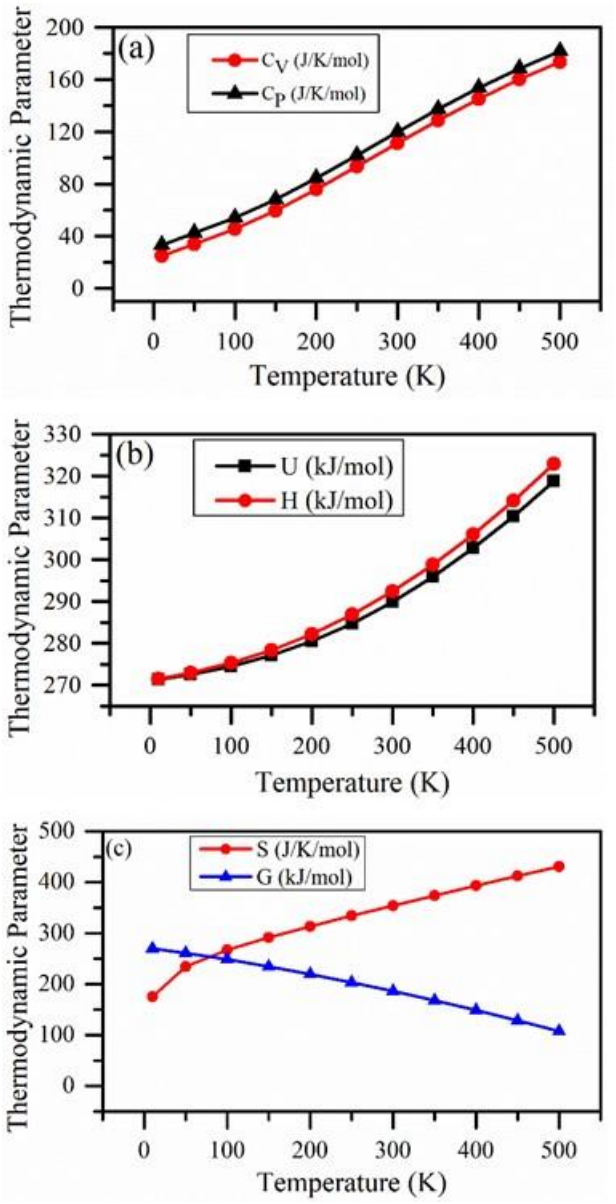


***Figure 9**: Temperature dependence of (a) heat capacity at constant volume and heat capacity at constant pressure, (b) internal energy and enthalpy, (c) entropy and Gibb's free energy*

**Thermodynamic parameter analysis**

To get the thermodynamic parameter of molecule, we use the DFT B3LYP/6-311++G (d, p) basis set followed by Moltran software. **Fig. 9(a)** shows the graph between heat capacity at constant volume ($C_V$) and heat capacity at constant pressure ($C_P$) with change in temperature. From the **Fig. 9(a)** for this $C_6H_5NO_2$ molecule, it is seen that the $C_V$ and $C_P$ are gradually increased with rise in temperature from 10 K to 500 K. **Fig. 9(b)** shows the internal energy (U) and enthalpy (H) with change in temperature. The thermodynamic parameters i.e. internal energy (U) and enthalpy (H) also increase with increasing temperature. **Fig. 9(c)** represents the graph of entropy (S) and Gibbs free energy (G) with change in temperature in the given range of 10 K to 500 K. In this figure, with the rise in temperature, the entropy increases. However, the Gibbs free energy decreases with the same rise in temperature. In the initial phase, entropy of the system rapidly increases and after that, it gradually increases with increasing temperature. The decrease in Gibbs free energy is attributed to its dependence on entropy, whereby an increase in entropy leads to a decrease in Gibbs free energy [41]. This change in entropy indicates that the atom possesses greater adaptability to adjust its thermodynamic system with respect to temperature variations [42，43].

## Conclusions

In this study, we investigated the Niacin molecule's optimized structure, vibration analysis in FT-IR spectrum, MEP, ED, ESP, HOMO-LUMO energy gap, DOS, global reactivity, Mulliken atomic charges and thermodynamic parameter analysis by using first-principles DFT/B3LYP method with a 6-311++G (d, p) basis set. To have optimal stabilized energy (-436.987 Hartree) and full optimization, title molecules went through nine optimization steps. There are 36 modes of vibration which are present at in-plane vibration and out-of-plane vibration. In Niacin molecule, the peak values from FT-IR spectrum for C=C are at 1448 $cm^{-1}$, 1632 $cm^{-1}$, for C-C is at 1358 $cm^{-1}$, for C-H stretching vibration are at 3152 $cm^{-1}$, 3184 $cm^{-1}$, 3202 $cm^{-1}$ also, for C-H in-plane bending vibration are at 1040 $cm^{-1}$, 1112 $cm^{-1}$, 1208 $cm^{-1}$, for C-H out-of-plane bending vibration are at 712 $cm^{-1}$ , 760 $cm^{-1}$, 792 $cm^{-1}$, 884 $cm^{-1}$, for C-O stretching vibration is at 1792 $cm^{-1}$, for C-N vibration are at 1292 $cm^{-1}$, 1449 $cm^{-1}$ and for O-H vibration is at 3768 $cm^{-1}$. The MEP and ESP map of the Niacin molecule showed that the oxygen and nitrogen atoms have the electrophilic region (yellow color) and the hydrogen atom have the nucleophilic region (blue color). ED presented the formation of electron bond (charge) distribution of the title molecule. The energy gap from HOMO-LUMO is found to be 5.398 eV and from DOS is 5.429 eV which is approximately equal. The Niacin molecule is hard due to the larger energy gap. The electronegativity value of 4.847 eV predicts the biological activity of Niacin derivatives based on their molecular structure and signifies the molecules ability to attract electron. The calculated value of chemical hardness is 2.7 eV which reflects the molecular stability and is likely to be more stable and less reactive in biological environments, maintaining its integrity and functionality. The softness value of 0.370 $eV^{-1}$ denotes the molecule polarizability. Also the chemical potential value is -4.847 eV which represent the ability to donate or accept electron. It provides critical insights into the molecule's reactivity, stability, interaction with biological targets, and overall role in metabolic processes. Electrophilic index with value 4.351 eV shows how niacin interacts with biological targets such as

enzymes or receptors, influencing binding affinity and specificity. From the calculation of Mulliken atomic charges distribution of the Niacin molecule, the C2 atom carries the greatest positive charge together with all the hydrogen atoms positioned on the upper side exhibiting positive charges too, while C1 bears the highest negative charge and C4, C5, N6, C11, O12, and O13 atoms located on the lower side demonstrate negative charges. The thermodynamic parameters such as $C_v$, $C_p$, U, H, and S were observed increasing upon increasing the temperature from 10 K to 500 K whereas G experiences a decreased in value in the same rise in temperature. We believe that our work makes a substantial contribution to the fields of biological chemistry and computational chemistry by offering solid databases and insights that are useful for drug development, toxicity, metabolic research, and teaching. Future research and development pertaining to Niacin and its derivatives is anticipated to be fueled by these resources, resulting in novel discoveries and uses in the medicines, healthcare, biology and chemistry.

## Acknowledgements

The authors are grateful to the Department of Physics, Patan Multiple Campus, Tribhuvan University, and the Department of Physics, St Xavier's College, Maitighar, Kathmandu, Nepal for needful help

## Author's Contribution Statement

**Chandra Budha:** Conceptualization, Writing – original draft, Methodology. **Krishna Bahadur Rai:** Review & editing, Investigation, Formal analysis, Data curation, Visualization, Validation, Resources, Supervision

## Conflict of Interest

The authors do not have any conflict of interest pertinent to this work.

## Data Availability Statement

The data that support the findings of this study can be made available from the corresponding author, upon reasonable request.

## References

1. J. B. Kirkland and M. L. Meyer-Ficca, *Advances in Food and Nutrition Research*, First Ed., Elsevier B. V., USA, 2018, Niacin, 83-149 (doi.org/10.1016/bs.afnr.2017.11.003)
2. S. H. Ganji, V. S. Kamanna and M. L. Kashyap, Niacin and cholesterol: role in cardiovascular disease, *The Journal of Nutritional Biochemistry*, 2003, 14(6), 298-305. (doi.org/10.1016/S0955-2863 (02)00284-X)
3. T. Chand and B. Savitri, Vitamin B3, *Industrial Biotechnology of Vitamins, Biopigments and Antioxidants*, First Edition, Wiley VCH, Germany, 2016, Vitamin B3, Niacin 41, 41-65. (doi.org/10.1002/9783527681754.ch3)
4. V. Gasperi, M. Sibilano, I. Savini and M. V. Catani, Niacin in the Central Nervous System, An Update of Biological Aspects and Clinical Applications, International *Journal of Molecular Sciences*, 2019, 20, 974. (doi.org/10.3390/ijms20040974)
5. J. Chen and M. Chopp, Niacin, an Old Drug, Has New Effects on Central Nervous System Disease, *The Open Drug Discovery Journal*, 2010, 2(1), 181-186. (doi.org/10.2174/1877381801002010181)
6. G. Karpagakalyaani, J. D. Magdaline & T. Chithambarathanu, Comparative spectral (FT-IR, FT-Raman, UV) investigations, HOMO–LUMO, NBO and in-silico docking analysis of Nikethamide, niazid and 2-Mercaptonicotinic acid, *Journal of Molecular Structure*, 2022, *1252*, 132032. (https://doi.org/10.1016/j.molstruc.2021.132032)
7. M. J. Saadh, F. A. Muhammad, R. Mahdavi, Y. N. Parizi, E. Balali, J. C. Cotrina-Aliaga, M. Adil, S. Ahjel, M. T. Churampi Arellano, Y. Gallardo-Lolandes, R. R. Maaliw III, M. Mirzaei and K. Harismah, Exploring impacts of oil and water environ-

ments on structural and electronic features of vitamin B3 along with DFT calculations, *Journal of Medicinal and Chemical Science*, 2023, 6(10), 2419–2431. (doi.org/10.26655/JMCHEMSCI.2023.10.17)

8. C. R. T. Kumari, M. Nageshwari, R. G. Raman and M. L. Caroline, Crystal growth, spectroscopic, DFT computational, and third harmonic generation studies of nicotinic Acid, *Journal of Molecular Structure,* 2018, 1163, 137–146. (doi.org/10.1016/j.molstruc.2018.02.091)
9. F. Bardak, Investigation of electronic structure-bioactive nature relation in niacin derivates by DFT calculations and molecular Docking, *Celal Bayar University Journal of Science*, 2017, 13(2), 333–342. (doi.org/10.18466/cbayarfbe.319815)
10. M. R. Hudson, D. G. Allis and B. S. Hudson, The inelastic neutron scattering spectrum of nicotinic acid and its assignment by solid-state density functional theory. *Chemical Physics Letters*, 2009, 473(1-3), 81–87. (doi.org/10.1016/j.cplett.2009.03.052)
11. H. R. K. Gauli, K. B. Rai, K. Giri and R. Neupane, Monte-carlo simulation of phase transition in 2d and 3d ising model, *Scientific World*, 2023, 16(16), 12–20. (doi.org/10.3126/sw.v16i16.56744)
12. S. Seshadri and M. P. Rasheed, Simulation of FTIR-IR and FTIR-Raman spectra based on scaled DFT calculations, vibrational assignments, hyperpolarizability, NMR chemical shifts and homo-lumo analysis of 1-chloro-4-nitrobenzene, International *Journal for Research in Applied Science and Engineering Technology*, 2017, 4(5), 632–649. (doi.org/10.13140/RG.2.2.26962.04809)
13. A. A. El-Saady, N. Roushdy, A. A. M. Farag, M. M. El-Nahass and D. M. Abdel Basset, Exploring the molecular spectroscopic and electronic characterization of nanocrystalline metal-free phthalocyanine: A DFT investigation, *Optical and Quantum Electronics*, 2023, 55(7), 662. (doi.org/10.1007/s11082-023-04877-8)
14. S. Gunasekaran, S. Kumaresan, R. Arunbalaji, G. Anand and S. Srinivasan, Density functional theory study of vibrational spectra, and assignment of fundamental modes of dacarbazine, *Journal of Chemical Sciences*, 2008, 120, 315–324. (doi.org/10.1007/s12039-008-0054-8)
15. G. Socrates, Infrared and Raman Characteristic Group Frequencies: Tables and Charts George Socrates John Wiley & Sons, *Journal of Raman Spectroscopy*, 2004, 35(10), 905. (doi.org/10.1002/jrs.1238)
16. T. Ojha, S. Limbu, P. M. Shrestha, S. P. Gupta and K. B. Rai, Comparative computational study on molecular structure, electronic and vibrational analysis of vinyl bromide based on HF and DFT approach, *Himalayan Journal of Science and Technology*, 2023, 7(1), 38-49. (doi.org/10.3126/hijost.v7i1.61128)
17. S. Limbu, T. Ojha, R. R. Ghimire and K. B. Rai, An investigation of vibrational analysis, thermodynamics properties and electronic properties of Formaldehyde and its stretch by substituent acetone, acetyl chloride and methyl acetate using First Principles analysis, *BIBECHANA*, 2024, 21(1), 23–36. (doi.org/10.3126/bibechana.v21i1.58684)
18. A. Atac, M. Karabacak, C. Karaca and E. Kose, NMR, UV, FT-IR, FT-Raman spectra and molecular structure (monomeric and dimeric structures) investigation of nicotinic acid N-oxide: A combined experimental and theoretical study, *Spectrochimica Acta Part A: Molecular and Biomolecular Spectroscopy*, 2012, 85(1), 145-154. (doi.org/10.1016/j.saa.2011.09.048)
19. V. Arjunan, P. S. Balamourougane, S. T. Govindaraja and S. Mohan, A comparative study on vibrational, conformational and electronic structure of 2-(hydroxymethyl) pyridine and 3-(hydroxymethyl) pyridine, *Journal of Molecular Structure*, 2012, 1018, 156-170. (doi.org/10.1016/j.molstruc.2012.03.017)
20 M. Kumar and R.A. Yadav, Experimental IR and Raman spectra and quantum chemical studies of molecular structures, conformers and vibrational characteristics of nicotinic acid and its N-oxide, Spectrochimica Acta Part A: *Molecular and Biomolecular Spectroscopy*, 2011, 79, 1316–1325

21. M. Baranska, M. Roman & K. Majzner, General overview on vibrational spectroscopy applied in biology and medicine, *Optical Spectroscopy and Computational Methods in Biology and Medicine*, 2014, 3-14. (https://doi.org/10.1007/978-94-007-7832-0_1)
22. R. Yankova, S. Genieva, N. Halachev and G. Dimitrova, Molecular structure, vibrational spectra, MEP, HOMO-LUMO and NBO analysis of Hf $(SeO_3)(SeO_4)(H_2O)$ 4, *Journal of Molecular Structure*, 2016, 1106, 82-88. (doi.org/10.1016/j.molstruc.2015.10.091)
23. R. Raju, C. Y. Panicker, P. S. Nayak, B. Narayana, B. K. Sarojini, C. Van Alsenoy and A. A. Al-Saadi, FT-IR, Molecular structure, first order hyperpolarizability, MEP, HOMO and LUMO analysis and NBO Analysis of 4-[(3-Acetylphenyl) Amino]-2-Methylidene-4-Oxobutanoic Acid, *Spectrochimica Acta Part A: Molecular and Biomolecular Spectroscopy*, 2015, 134, 63-72. (doi.org/10.1016/j.saa.2014.06.051)
24. F. Basha, F. L. A. Khan, S. Muthu and M. Raja, Computational evaluation on molecular structure (Monomer, Dimer), RDG, ELF, electronic (HOMO-LUMO, MEP) properties, and spectroscopic profiling of 8-Quinolinesulfonamide with molecular docking studies, *Computational and Theoretical Chemistry,* 2021, 1198, 113169. (doi.org/10.1016/j.comptc.2021.113169)
25. J. C. Prasana, S. Muthu and C. S. Abraham, Molecular docking studies, charge transfer excitation and wave function analyses (ESP, ELF, LOL) on valacyclovir: a potential antiviral drug, C*omputational Biology and Chemistry*, 2019, 78, 9–17. (doi.org/10.1016/j.compbiolchem.2018.11.014)
26. B. Shivaleela, G. G. Shivraj and S. M. Hanagodimath, Estimation of dipole moments by solvatochromic shift method, spectroscopic analysis of UV–Visible, HOMO-LUMO, ESP Map, Mulliken atomic charges, NBO and NLO properties of benzofuran derivative, *Results in Chemistry*, 2023, 6, 101046. (doi.org/10.1016/j.rechem.2023.101046)
27. S. Basavaraj, S. G. Gounhalli, O. Patil and S. M. Hanagodimath, Quenching of fluorescence, dipole moments and DFT studies of newly synthesized amino-thiadiazole coumarin derivative, *Journal of the Maharaja Sayajirao University of Baroda,* 2021, 55(1), 200-218.
28. P. Sjoberg & P. Politzer, Use of the electrostatic potential at the molecular surface to interpret and predict nucleophilic processes. *Journal of Physical Chemistry*, 1990, 94(10), 3959-3961. (https://doi.org/10.1021/j100373a017)
29. M. B. Smith and J. March, March's *Advanced Organic Chemistry: Reactions, Mechanisms, and Structure*, Sixth Edition, Wiley, 2007
30. D. Voet, J. G. Voet and C. W. Pratt, *Fundamentals of Biochemistry: Life at the Molecular Level*. Fifth Edition, Wiley, 2016
31. G. A. Jeffrey, *An Introduction to Hydrogen Bonding*. Oxford University Press, 1997
32. B. D. Joshi, P. Tandon and S. Jain, Structure, MESP and HOMO-LUMO Study of 10-Acetyl-10H-Phenothiazine 5-Oxide using vibrational spectroscopy and quantum chemical methods, *BIBECHANA*, 2013, 9, 38–49.
33. P. S. Kumar, K. Vasudevan, A. Prakasam, M. Geetha and P. M. Anbarasan, Quantum chemistry calculations of 3-phenoxyphthalonitrile dye sensitizer for solar cells, *Spectrochimica Acta Part A*, 2010, 77(1), 45–50. (doi.org/10.1016/j.saa.2010.04.021)
34. R. M. Issa, M. K. Awad and F. M. Atlam, Quantum chemical studies on the inhibition of corrosion of copper surface by substituted uracils, *Applied Surface Science*, 2008, 255(5). 2433-2441. (doi.org/10.1016/j.apsusc.2008.07.155)
35. P. S. Ganesh, S. Y. Kim, D. S Choi, S. Kaya, G Serdaroglu, G. Shimoga, E. J. Shin and S. H. Lee, Electrochemical investigationsand theoretical studies of biocompatible niacin-modified carbon paste electrodeinterface for electrochemical sensing of folicacid, anesh, *Journal of Analytical Science and Technology*, 2021, 12(47), 1-14.

(https://doi.org/10.1186/s40543-021-00301-6)

36. R. P. Yadav, K. B. Rai and S. P. Shrestha, Electrical and optical properties of dip coated Al-doped ZnO thin films: effect of Al-concentration, starting solution and sample ageing, *Mongolian Journal of Chemistry*, 2021, 22(48) 38-44. (doi.org/10.5564/mjc.v22i48.1743)
37. I. B. Khadka, K. B. Rai, M. M. Alsardia, B. U. Haq and S. H. Kim, Raman investigation of substrate-induced strain in epitaxially grown graphene on low/high miscut angled silicon carbide and its application perspectives, *Optical Materials*, 2023, 140, 113836. (doi.org/10.1016/j.optmat.2023.113836)
38. B. Shivaleela, G. G. Shivraj and S. M. Hanagodimath, Estimation of dipole moments by solvatochromic shift method, spectroscopic analysis of UV–Visible, HOMO-LUMO, ESP Map, Mulliken atomic charges, NBO and NLO Properties of benzofuran derivative, *Results in Chemistry*, 2023, 6, 101046. (doi.org/10.1016/j.rechem.2023.101046)
39. E. Ç. Kaya, A. A. Kaya, Z. Demircioğlu and O. Buyukgungor, Synthesis, spectroscopic characterization, X-ray Structure and DFT Calculations of Ni(II) Bis(3,4-Dimethoxybenzoate) Bis(Nicotinamide) Dihydrate, *Heterocyclic Communications*, 2017, 23(2), 115–123. (doi.org/10.1515/hc-2016-0099)
40. K. B. Rai, R. R. Ghimire, C. Dhakal, K. Pudasainee and B. Siwakoti, Structural equilibrium configuration of benzene and aniline: a first-principles study, *Journal of Nepal Chemical Society*, 2024, 44(1), 1–15. (doi.org/10.3126/jncs.v44i1.62675)
41. B. Raja, B. V. Balachandran, B. Revanthi and K. Anitha, Molecular structure vibrational spectroscopic natural bond orbital analysis, frontier molecules orbital analysis and thermodynamics properties of n-tert-Butoxy carbonyll-phenylalanine by DFT methods, *Materials Research Innovations*, 2019, 23(6), 330–334. (doi.org/10.1080/14328917.2018.1477544)
42. R. Ghimire, A. Rana Magar, B. Basnet, R. Uprety, K. Pudasainee and K. B. Rai, Study of the spectroscopic analysis, electronic structures and thermodynamic properties of ethyl benzene using first-principles density functional theory, Contemporary Research: An Interdisciplinary Academic Journal, 2024, 7(1), 80-99 (https://doi.org/10.3126/craiaj.v7i1.67259)
43 R. Ramaiyan, S. Seshadri, Spectroscopic electronic structure and HOMO-LUMO analysis of 4-Bromo-2-Fluoro-1-Nitrobenzene, International Journal of Advance Research, 2017, 5(5), 87–100.